REPORT DOCUMENTATION PAGE

Form Approved OMB NO. 0704-0188

The public reporting burden for this collection of information is estimated to average 1 hour per response, including the time for reviewing instructions, searching existing data sources, gathering and maintaining the data needed, and completing and reviewing the collection of information. Send comments regarding this burden estimate or any other aspect of this collection of information, including suggesstions for reducing this burden, to Washington Headquarters Services, Directorate for Information Operations and Reports, 1215 Jefferson Davis Highway, Suite 1204, Arlington VA, 22202-4302. Respondents should be aware that notwithstanding any other provision of law, no person shall be subject to any oenalty for failing to comply with a collection of information if it does not display a currently valid OMB control number.
PLEASE DO NOT RETURN YOUR FORM TO THE ABOVE ADDRESS.

1. REPORT DATE (DD-MM-YYYY)	2. REPORT TYPE	3. DATES COVERED (From - To)
10-09-2013	Final Report	15-Apr-2009 - 14-Apr-2013

4. TITLE AND SUBTITLE
Nanocomposites

5a. CONTRACT NUMBER
W911NF-09-1-0145

5b. GRANT NUMBER

5c. PROGRAM ELEMENT NUMBER
611102

6. AUTHORS
Michael E. Mackay, PhD

5d. PROJECT NUMBER

5e. TASK NUMBER

5f. WORK UNIT NUMBER

7. PERFORMING ORGANIZATION NAMES AND ADDRESSES
University of Delaware
210 Hullihen Hall

Newark, DE 19716 -0099

8. PERFORMING ORGANIZATION REPORT NUMBER

9. SPONSORING/MONITORING AGENCY NAME(S) AND ADDRESS(ES)
U.S. Army Research Office
P.O. Box 12211
Research Triangle Park, NC 27709-2211

10. SPONSOR/MONITOR'S ACRONYM(S)
ARO

11. SPONSOR/MONITOR'S REPORT NUMBER(S)
55967-CH.1

12. DISTRIBUTION AVAILIBILITY STATEMENT
Approved for Public Release; Distribution Unlimited

13. SUPPLEMENTARY NOTES
The views, opinions and/or findings contained in this report are those of the author(s) and should not contrued as an official Department of the Army position, policy or decision, unless so designated by other documentation.

14. ABSTRACT
: Direct reinforcement of composite materials is typically promoted through use of high aspect ratio, stiff inclusions whose interface is modified to mediate stress transfer. Here a markedly different mechanism, indirect reinforcement, is achieved through use of weakly-interacting, spherical nanoparticles. Mechanical property enhancement is achieved by nanoparticles introducing density fluctuations to affect the polymer packing near their interface. This results in two phenomena; first a lower bulk modulus is found meaning the material becomes more

15. SUBJECT TERMS
nanocomposite, polymer, rheology, tensile modulus

16. SECURITY CLASSIFICATION OF:			17. LIMITATION OF ABSTRACT	15. NUMBER OF PAGES	19a. NAME OF RESPONSIBLE PERSON
a. REPORT	b. ABSTRACT	c. THIS PAGE			Michael Mackay
UU	UU	UU	UU		19b. TELEPHONE NUMBER: 302-831-6194

Report Title

Nanocomposites

ABSTRACT

: Direct reinforcement of composite materials is typically promoted through use of high aspect ratio, stiff inclusions whose interface is modified to mediate stress transfer. Here a markedly different mechanism, indirect reinforcement, is achieved through use of weakly-interacting, spherical nanoparticles. Mechanical property enhancement is achieved by nanoparticles introducing density fluctuations to affect the polymer packing near their interface. This results in two phenomena; first a lower bulk modulus is found meaning the material becomes more compressible. Secondly, the tensile modulus increases. The first phenomenon occurs (we think) because the nanoparticle is surrounded by a low density region. The second is due to high density regions surrounding the low density promoting a higher tensile modulus.

We have considered many new nanoparticle systems and have had to take a very careful route to ensure the results we have obtained are not spurious. We reproduced most previous results conducted by a previous student in the group since some results were found to be at fault and are sure what we have now measured are correct. Several manuscripts are now in preparation.

Enter List of papers submitted or published that acknowledge ARO support from the start of the project to the date of this printing. List the papers, including journal references, in the following categories:

(a) Papers published in peer-reviewed journals (N/A for none)

Received Paper

TOTAL:

Number of Papers published in peer-reviewed journals:

(b) Papers published in non-peer-reviewed journals (N/A for none)

Received Paper

TOTAL:

Number of Papers published in non peer-reviewed journals:

(c) Presentations

Number of Presentations: 3.00

Non Peer-Reviewed Conference Proceeding publications (other than abstracts):

Received Paper

TOTAL:

Number of Non Peer-Reviewed Conference Proceeding publications (other than abstracts):

Peer-Reviewed Conference Proceeding publications (other than abstracts):

Received Paper

TOTAL:

Number of Peer-Reviewed Conference Proceeding publications (other than abstracts):

(d) Manuscripts

Received Paper

TOTAL:

Number of Manuscripts:

Books

Received Paper

TOTAL:

Patents Submitted

Patents Awarded

Awards

Graduate Students

NAME	PERCENT_SUPPORTED	Discipline
J. J. Wie	1.00	
FTE Equivalent:	**1.00**	
Total Number:	**1**	

Names of Post Doctorates

NAME	PERCENT_SUPPORTED
FTE Equivalent:	
Total Number:	

Names of Faculty Supported

NAME	PERCENT_SUPPORTED	National Academy Member
Michael E. Mackay	0.00	
FTE Equivalent:	**0.00**	
Total Number:	**1**	

Names of Under Graduate students supported

NAME	PERCENT_SUPPORTED
FTE Equivalent:	
Total Number:	

Student Metrics

This section only applies to graduating undergraduates supported by this agreement in this reporting period

The number of undergraduates funded by this agreement who graduated during this period:	0.00
The number of undergraduates funded by this agreement who graduated during this period with a degree in science, mathematics, engineering, or technology fields:.....	0.00
The number of undergraduates funded by your agreement who graduated during this period and will continue to pursue a graduate or Ph.D. degree in science, mathematics, engineering, or technology fields:.....	0.00
Number of graduating undergraduates who achieved a 3.5 GPA to 4.0 (4.0 max scale):	0.00
Number of graduating undergraduates funded by a DoD funded Center of Excellence grant for Education, Research and Engineering:	0.00
The number of undergraduates funded by your agreement who graduated during this period and intend to work for the Department of Defense	0.00
The number of undergraduates funded by your agreement who graduated during this period and will receive scholarships or fellowships for further studies in science, mathematics, engineering or technology fields:	0.00

Names of Personnel receiving masters degrees

NAME
Total Number:

Names of personnel receiving PHDs

NAME
J. J. Wie
Total Number: 1

Names of other research staff

NAME	PERCENT_SUPPORTED
FTE Equivalent:	
Total Number:	

Sub Contractors (DD882)

Inventions (DD882)

Scientific Progress

See attachment

Technology Transfer

Summary: Direct reinforcement of composite materials is typically promoted through use of high aspect ratio, stiff inclusions whose interface is modified to mediate stress transfer. Here a markedly different mechanism, indirect reinforcement, is achieved through use of weakly-interacting, spherical nanoparticles. Mechanical property enhancement is achieved by nanoparticles introducing density fluctuations to affect the polymer packing near their interface. This results in two phenomena; first a lower bulk modulus is found meaning the material becomes more compressible. Secondly, the tensile modulus increases. The first phenomenon occurs (we think) because the nanoparticle is surrounded by a low density region. The second is due to high density regions surrounding the low density promoting a higher tensile modulus.

We have considered many new nanoparticle systems and have had to take a very careful route to ensure the results we have obtained are not spurious. We reproduced most previous results conducted by a previous student in the group since some results were found to be at fault and are sure what we have now measured are correct. Several manuscripts are now in preparation.

Discussion: Dispersion of the nanoparticles into the polymer is a critical step. Figure 1 below shows how we did this. The nanoparticles and polymer were dissolved in a good solvent then precipitated into a mutual non-solvent and the precipitant was dried for a week at 40°C. An 8 mm diameter disk was formed under vacuum in a modified FT-IR pellet press and then characterization could be performed, such as with the Rigaku Ultima IV Small Angle X-Ray Scattering (SAXS) instrument in our laboratory.

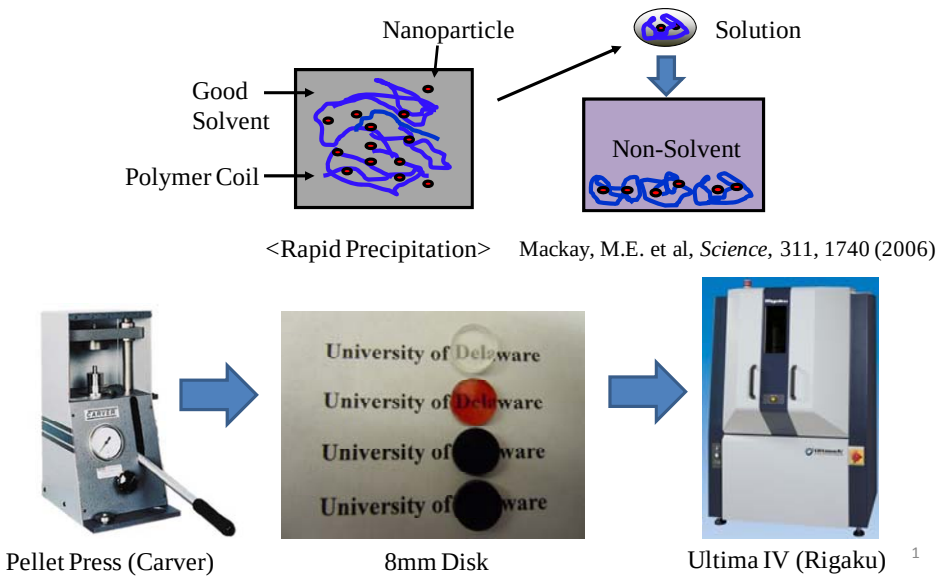

Figure 1: Description of the dispersion process required to make a homogeneous blend of nanoparticles in a polymer.

We used the SAXS data to determine the degree of nanoparticle dispersion in our systems with data given in Figure 2. The overall scattering intensity (I) as a function of wave vector (q) is consistent with well dispersed blends for both an industrial 10 nm magnetite nanoparticle system (EMG1300, FerroTech) and smaller 5 nm magnetite system synthesized in the group of Prof. J. Pyun at the University of Arizona.

SAXS measurements were carried out to estimate the interaction between particles and thermodynamic stability in polymer blends using Zimm plots. Equation 1 was used to construct SAXS Zimm plots containing electron density contrast ($\Delta\rho_e$) as an adjustable parameter

$$\frac{\phi_c V_c}{I(q,\phi_c)} = \left[1 + \frac{5}{9}\left(\frac{q d_z}{2}\right)^2\right]\left[\frac{1}{\Delta\rho_e{}^2} + \frac{8\bar{B}_2}{\Delta\rho_e{}^2}\phi_c\right] \qquad (1)$$

The other parameters are defined in the original publication[1] with the important ones for this report being the Z-average diameter (d_z) and the second virial coefficient ($\bar{B}_2$).

The thermodynamic stability of nanoparticles in a polymer melt is essential to ensure good dispersion during the annealing process. Annealing is required before rheological and mechanical measurements are performed to achieve thermodynamically equilibrated states. Then, SAXS measurements were carried out at 25 °C, 170 °C, and 30 °C at the Advanced Photon Source (APS). No significant difference in the scattering profiles and thermodynamic parameters were found for all three measurement temperatures as shown in Figure 2 and Table 1. This demonstrates that quenching the nanocomposite from the annealing temperature (which is representative of the processing temperature if a product were being made) effectively freezes the thermodynamic state.

Here, the second virial coefficient was made dimensionless by normalizing with the hard sphere value. Positive B_2 values indicate thermodynamic stability of magnetite nanoparticles in polystyrene which is critical to the success in making true nanocomposites.

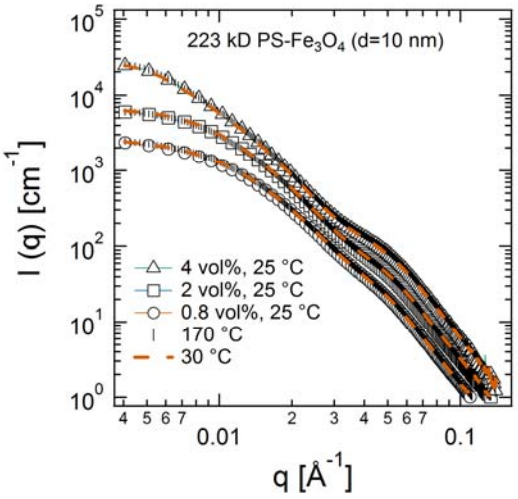

Figure 2: Small angle X-ray scattering profiles of 223 kD PS - Fe_3O_4 (d=10 nm) nanocomposites at different measurement temperatures.

Table 1. Zimm plot results at different measurement temperatures for 223 kD PS-Fe_3O_4 (d=10 nm) nanocomposites.

Measurement Temperature	d_z (nm)	$\Delta\rho_e$ x 10^{11} (cm^{-2})	$\overline{B_2}$	ε (k_BT)
25 °C	28.7±0.4	2.35 ± 0.01	0.0042 ± 0.0002	0.35
170 °C	26.0±1.7	2.38± 0.03	0.0046 ± 0.0001	0.35
30 °C	27.5±2.7	2.37 ± 0.04	0.0041 ± 0.0001	0.35

Since the ambient measurement conditions could capture the thermodynamic stability of the polymer melts, by quenching pre-annealed polymer nanocomposites, the rest of the systems in this study were measured at room temperature after quenching the pre-annealed nanocomposites using a Rigaku Ultima IV X-ray instrument. The Zimm plot results of 393 kD PS systems are summarized in Table 2.

Table 2. Zimm plot results measured at 25ºC for 393 kD PS-Fe_3O_4 (d=5 and 10 nm) nanocomposites.

PS MW (kD)/ Fe_3O_4 d (nm)	$d_{z,DLS}$ (nm)	$d_{z,SAXS}$ (nm)	$\Delta\rho_e$ x 10^{11} (cm^{-2})	$\overline{B_2}$	ε (k_BT)
393/ 5	8.7 ± 2.1	8.8 ± 0.9	3.81 ± 0.27	0.0258 ± 0.0018	0.34
393/ 10	18.8 ± 7.5	18.0 ± 1.0	2.03 ± 0.11	0.0583 ± 0.0033	0.33

The z-averaged diameter of the 393 kD-nanoparticle systems are almost equal to those extracted from dynamic light scattering experiments, suggesting this system exhibits minimal clustering and is thermodynamically stable.

For reference, Transmission Electron Micrographs (TEMs) shown in Figure 3 also supported the finding from SAXS. Good dispersion was found for lower concentrations however a significant amount of clustering was found at higher nanoparticle concentrations.

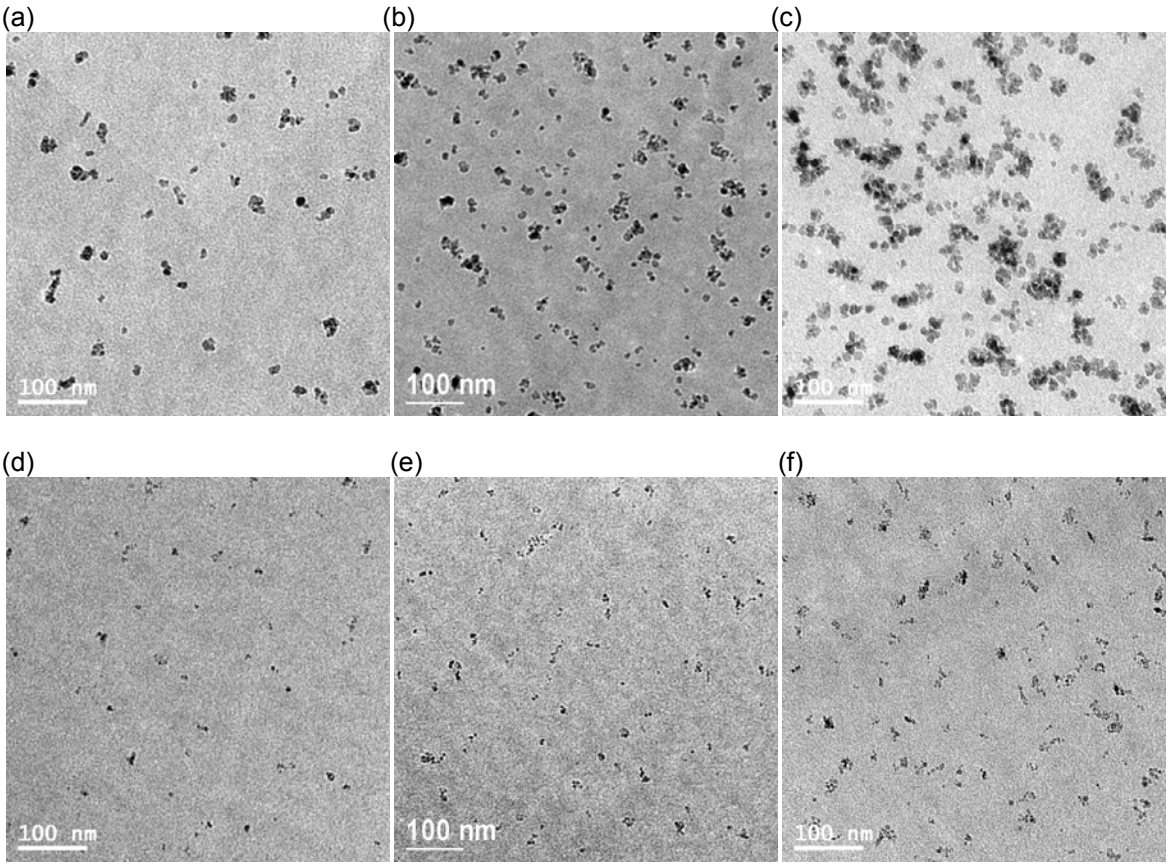

Figure 3: 393 kD polystyrene nanocomposites with 10 and 5 nm iron oxide nanoparticles (a) 0.8 vol% Fe_3O_4 (d=10 nm) (b) 2 vol% Fe_3O_4 (d=10 nm) (c) 4 vol% Fe_3O_4 (d=10 nm) (d) 0.2 vol% Fe_3O_4 (d=5 nm) (e) 0.4 vol% Fe_3O_4 (d=5 nm) (f) 0.8 vol% Fe_3O_4 (d=5 nm)

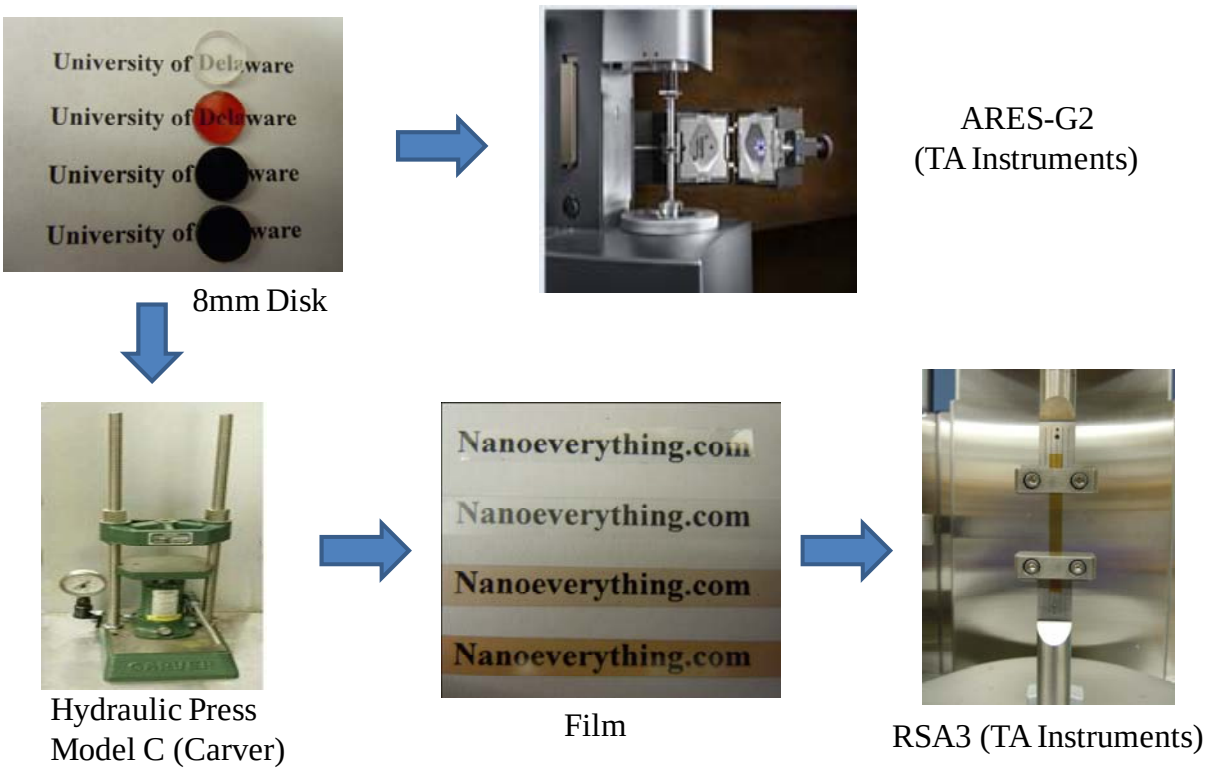

Figure 4: Preparation of samples for melt rheological testing (ARES-G2) or tensile testing (RSA3).

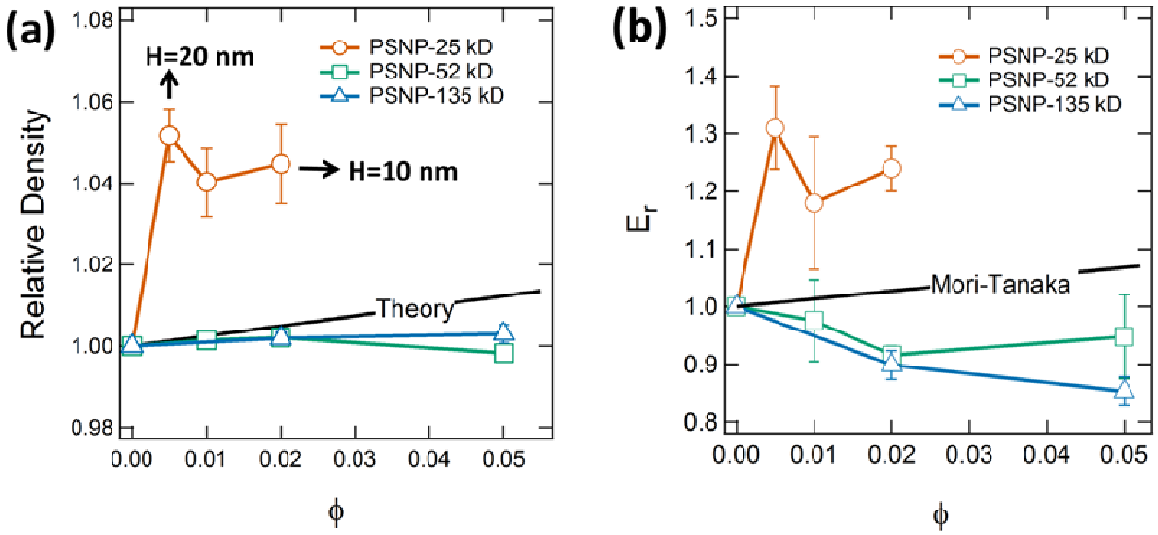

Figure 5: (a) Relative density of three different molecular weights of PSNP systems accurately determined by a Helium gas pycnometer at room temperature (~ 25 °C). Theory indicates theoretical value calculated from the polymer and nanoparticle density information. H is interparticle distance between nanoparticles. (b) Relative tensile modulus of 393 kD PS nanocomposites against nanoparticle volume fraction. Mori-Tanaka indicates predicted values by a conventional continuum micromechanics model.

Disks for tensile testing were pressed to make films as shown in Figure 4. Results from the tensile testing experiments are shown in Figure 5. Nanoparticle volume fractions were corrected by measuring the density of polymer and nanoparticles. Here it is found that nanoparticles having a size of 3 – 5 nm provide the best reinforcement at low volume fraction. Our hypothesis is that as the size of the nanoparticle approaches the persistence length of the polymer (~ 3 nm for polystyrene) The polymer can not effectively pack around the particle. When this happens the polymer has density fluctuations within the bulk material.

We know the density fluctuations occur since we find the nanocomposites become more compressible, as described in the previous interim report, and an increase in compressibility means the formation of void region. The introduction of voidage without formation of high density regions for PS nanoparticle (PSNP) systems should produce a slight density reduction regardless of molecular weight since PSNPs have a density of 1.30 g/cc which is a little higher than linear polystyrene 1.05 g/cc. However, the results in Figure 5a shows the nanocomposite density remaining essentially unchanged for 52 kD and 135 kD PSNPs, suggesting that any voids had been compensated by the higher density regions. Remarkably, the inclusion of 25 kD PSNP resulted in significant densification, which is indicative of a large amount of high density regions and/or substantially high density for high density regions.

The relative tensile modulus results of 393 kD PS nanocomposites against nanoparticle volume fraction are presented in Figure 5b. The PSNP can yield a large reinforcement or a reduction depending on their molecular weight (25, 52, or 135 kD). General trend of tensile modulus was similar to density results shown in Figure 5a. In uniaxial tension, here we offer a continuum explanation of how it may be possible to have a tensile modulus increase. Consider first where there is no density fluctuations as shown in Figure 6a. There are three regions that operate in series and parallel to yield the following tensile modulus, E,

$$\frac{1}{E} = \frac{\phi_{m1}}{E_m} + \frac{\phi_2}{\phi^*_{m2}E_m + \phi^*_{NP}E_{NP}} + \frac{\phi_{m3}}{E_m} \tag{2}$$

Here, E_m and E_{NP} are the matrix and nanoparticle modulus, respectively. We note the volume fraction of the matrix in region 1 (ϕ_{m1}) is equal to that in region 3 (ϕ_{m3}) where

$$\phi_{m1} = \phi_{m3} = \frac{[H+d]^2\frac{H}{2}}{[H+d]^3} = \frac{1}{2}\frac{H}{H+d} \tag{3}$$

The distance between the nanoparticle surfaces is given by

$$\frac{H}{d} = \left[\frac{1}{\phi_{NP}}\right]^{1/3} - 1 \tag{4}$$

where ϕ_{NP} is the nanoparticle volume fraction. One can now write

$$\phi_{m1} = \phi_{m3} = \frac{1}{2}\left[1 - {\phi_{NP}}^{1/3}\right] \tag{5}$$

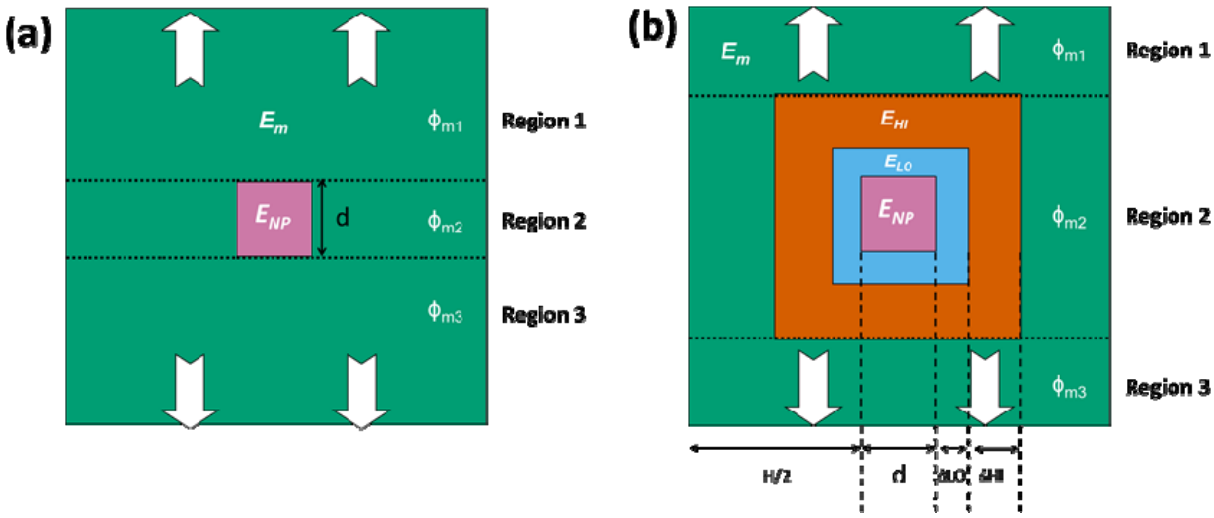

Figure 6: (a) Cartoon showing the tension of the matrix without presence of interfacial components. (b) Cartoon showing the tension of the matrix with presence of the high density and low density regions

The volume fraction of region 2, ϕ_2, is equal to

(6)

where ϕ_{m2} and ϕ_{NP} are the matrix volume fraction of the matrix in region 2 and the nanoparticle volume fraction, respectively. We find

- (7)

Since the nanoparticle and matrix operate in parallel in region 2, the modulus in that region, E_2, is

(8)

where the superscript * represents the relative amount of each component within that region

———— = 1- , ———— (9)

we can now write

– ——— ———————————— (10)

This model agrees fairly well with contemporary continuum models, however, we use this to understand how a high density region can provide reinforcement as well as the sensitivity of the modulus to nanoparticle diameter and not its ability to accurately predict the tensile modulus.

To this end we now consider the cartoon in Figure 6b. We make the further assumption that in region 2 only the matrix and high density region contribute. This is equivalent to assuming the high density region provides reinforcement like a table tennis ball where the material within it does not contribute.

Physically one may expect this if the low density region does not transfer stress to the nanoparticle. Considering the three regions we find

(11)

where E_{HI} is the high density regions tensile modulus and ϕ'_{NP} an effective nanoparticle volume fraction

(12)

where ΔLO and ΔHI are the low and high density regions' thickness.

Figure 6b shows a nanoparticle surrounded with a low density then a high density region and equation 11 was used for the tensile modulus calculation. Note how dependent the effect is with diameter. Part of the decrease maybe due to changes in the molecular packing as the nanoparticles become larger, yet, the simple model we presented could explain some of it. Referring to Figure 7 one can see that near 5 nm there is a precipitous decrease in modulus with an increase in diameter. This is because the effective volume fraction scales with d^{-3} to promote such a decrease. Thus, a change in packing could be a factor in the modulus decrease, as evidenced by the density data in Figure 5, however, the reinforcement is very sensitive to diameter too which could lead to such sensitive behavior.

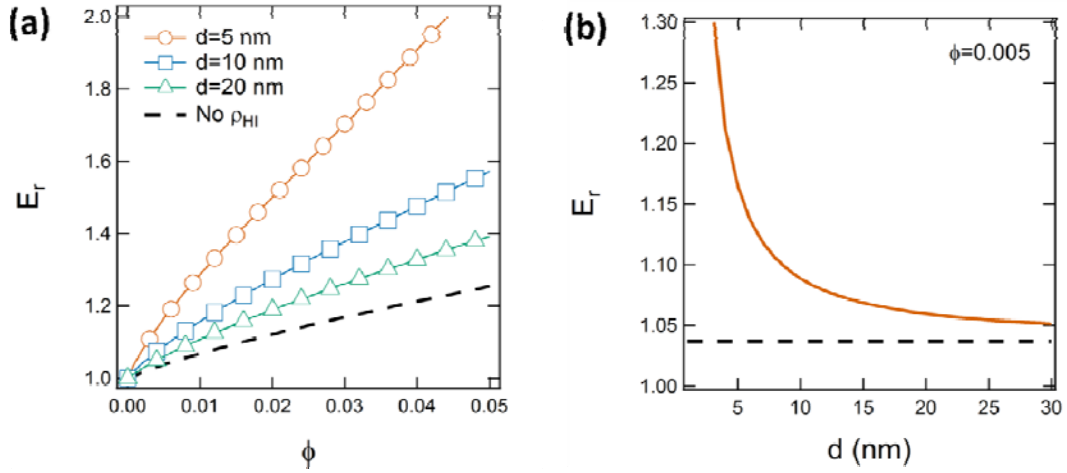

Figure 7: (a) The relative tensile modulus is plotted versus nanoparticle volume fraction for different particle diameter. Dashed line indicates relative tensile modulus prediction assuming no high density region formation. (b) The relative tensile modulus is plotted versus nanoparticle diameter at nanoparticle volume fraction ϕ=0.005. Dashed line indicates relative tensile modulus prediction assuming no high density region formation. In both figures Δ_{LO}=0.5 nm, Δ_{HI}=1.5 nm and E_{HI}=10.

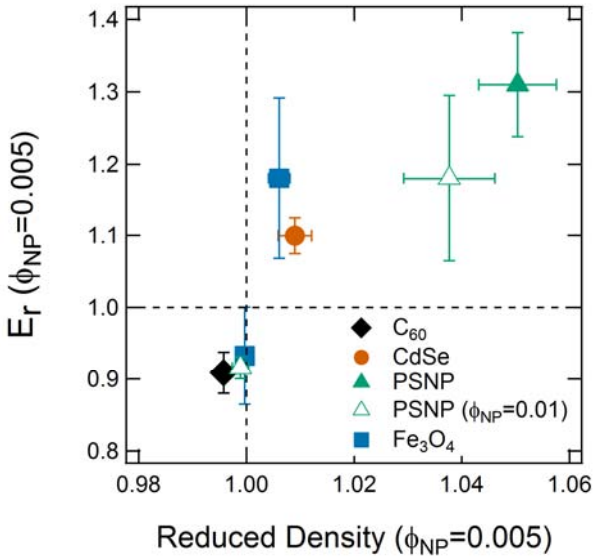

Figure 8. (a) The relative tensile modulus of 393 kD PS nanocomposites is plotted versus reduced density. The nanocomposites were prepared by the addition of various nanoparticles at □~0.005. Nanoparticle diameters for C_{60}, CdSe, and PSNP were 0.76 nm, 3 nm, and 5 nm, respectively. Unfilled triangles are PSNPs at □=0.01 and the PSNPs next to C_{60} had molecular weights of 52 kD while both top right two PSNPs had molecular weight of 25 kD. Fe_3O_4 nanoparticle next to C_{60} had 10 nm and one next to CdSe nanoparticle had 5 nm.

To further investigate the particle size effect on densification and tensile modulus reinforcement, different sized and type nanoparticles were studied in addition to PSNPs at a low nanoparticle volume fraction, □=0.005. The relative tensile modulus was plotted against reduced density and shown in Figure 5.7. Here, the reduced density is normalized by the theoretical density from the regular rule of mixtures by knowing the density information of the nanoparticle and polymer. Thus, a reduced density larger than unity indicates densification of polymer nanocomposites.

Fullerene (C_{60}) has a 0.76 nm diameter, which is hypothesized to be too small to perturb the polymer chain conformation and so little reinforcement or densification occurs. The iron oxide (Fe_3O_4) nanoparticle data point next to C_{60} in the figure had a 10 nm diameter and was hypothesized to be too large to distort the polymer chain similar to what was found with the larger PSNPs discussed above. The data for the 52 kD PSNP with a diameter of 6.2 nm (□=0.01) was also included in Figure 8 for comparison and the data point is next to the C_{60} data point in the figure. Neither demonstrated densification nor reinforcement. Meanwhile, the 3 nm diameter cadmium selenide (CdSe) and 5 nm Fe_3O_4 nanoparticles whose size is comparable to the polymer Kuhn length and both exhibited densification and reinforcement. Remarkably, the 5 nm diameter PSNP had the largest densification and reinforcement as Bedrov et al. reported maximized densification occurs at the athermal condition. [3] Although only a few nanoparticles having different chemical components were tested due to their limited availability, we have found a definite particle size dependent density and tensile modulus. The effect is subtle, yet, quite robust as various systems, inorganic or organic, produce the same phenomenon.

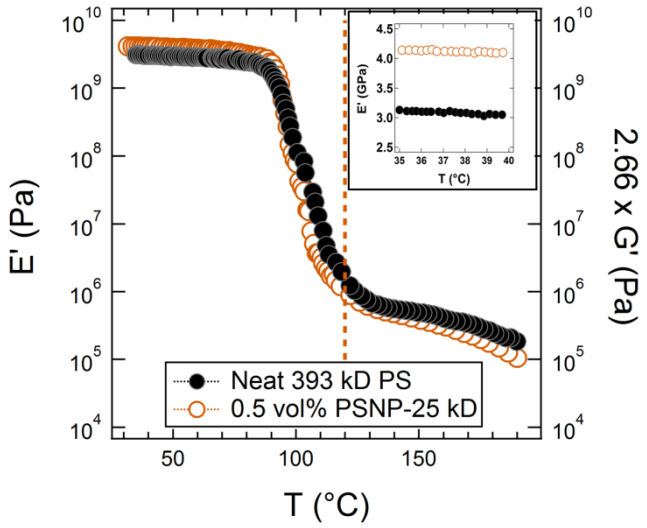

Figure 9. The inclusion of smallest PSNP enhanced mechanical properties in the glassy state while the melt viscosity decreased compared to neat PS. The E' is matched with G' at 120 °C with factor of 2.66 using the Poisson's ratio of 0.33 for PS as E=2G(1+v) where v is Poisson's ratio. The inset shows the magnified elastic storage modulus data in the glassy states.

We previously reported a melt viscosity decrease by the addition of PSNP's to linear PS matrices. Rheological characterization was performed with the nanocomposites to ensure whether the mechanical reinforcement in the glassy state is contradictory to the melt viscosity decrease. Polymer melt properties were probed using a torsional rheometer and matched with solid state properties determined with a dynamic mechanical analyzer (DMA) operating in tension. Measurements were taken at a frequency of 1 rad/s with both instruments. Compared to neat PS, an enhanced elastic storage modulus, E', in tension was found by the inclusion of 0.5 vol% 25 kD PSNP in the glassy state (Figure 9). However, E' around the polymer glass transition temperature (T_g) and shear storage modulus, G' above T_g of the nanocomposite became less than that of the pure polymer, suggesting a viscosity reduction in the liquid state. Therefore, reinforcement in the glassy state is not contradictory to previous findings of a melt viscosity decrease.

References

1. Anderson, B.J. and Zukoski, C.F., *Nanoparticle stability in polymer melts as determined by particle second virial measurement*, Macromolecules **40** (2007) 5133-5140.
2. Garcia-Fierro, J.L. and Aleman, J.V., *Interactions between water and polystyrene*, Euro Poly J **21** (1985) 753-756.
3. Bedrov, D., G.D. Smith, and J.S. Smith, *Matrix-induced nanoparticle interactions in a polymer melt: A molecular dynamics simulation study.* Journal of Chemical Physics, 2003. **119**(19): p. 10438-10447.